Neuron, Vol. 29, 33–44, January, 2001, Copyright ©2001 by Cell Press

Traveling Electrical Waves in Cortex: Insights from Phase Dynamics and Speculation on a Computational Role

Viewpoint

G. Bard Ermentrout*†‖ and David Kleinfeld‡§‖
*Department of Mathematics
†Department of Neurobiology
University of Pittsburgh
Pittsburgh, Pennsylvania 15260
‡Department of Physics
§Neurosciences Graduate Program
University of California, San Diego
La Jolla, California 92093

Summary

The theory of coupled phase oscillators provides a framework to understand the emergent properties of networks of neuronal oscillators. When the architecture of the network is dominated by short-range connections, the pattern of electrical output is predicted to correspond to traveling plane and rotating waves, in addition to synchronized output. We argue that this theory provides the foundation for understanding the traveling electrical waves that are observed across olfactory, visual, and visuomotor areas of cortex in a variety of species. The waves are typically present during periods outside of stimulation, while synchronous activity typically dominates in the presence of a strong stimulus. We suggest that the continuum of phase shifts during epochs with traveling waves provides a means to scan the incoming sensory stream for novel features. Experiments to test our theoretical approach are presented.

Stimulus-induced oscillations are a hallmark of neuronal dynamics in many sensory systems (Gray, 1994). In the visual system of mammals, oscillations occur along both sensory and sensorimotor limbs of the visual system (Roelfsema et al., 1997; Castelo-Branco et al., 1998). Furthermore, the magnitude and spatial extent of these oscillations are modulated by the nature of the visual stimulus (Eckhorn et al., 1988; Gray et al., 1989). Theoretical studies on networks of neuronal oscillators (Kuramoto, 1984; Kopell and Ermentrout, 1986) show that a form of oscillations known as traveling oscillatory waves are an emergent property of systems with spatially restricted connectivity. Examples that bear out these predictions are observed in multisite measurements across the central olfactory organs of some species (Freeman, 1978; Delaney et al., 1994; Lam et al., 2000), the visual system of turtle (Prechtl et al., 1997, 2000), and possibly throughout human cortex (Ribary et al., 1991; Kelso, 1995). Although traveling waves of electrical activity are usually not reported in studies on visual cortices of cat or monkey (i.e., the reported stimulus-induced electrical activity is coherent with no phase shift), recent evidence suggests that the apparent absence of waves is a consequence of the experimental paradigm (A. Gabriel and R. Eckhorn, 1999, Soc. Neurosci., abstract; M. Munk et al., 1999, Gottingen Neurobiol. Conf., abstract; M. Munk et al., 2000, Soc. Neurosci., abstract). In fact, the results of experiments with awake cat strongly suggest the presence of electrical waves in visuomotor cortices (Roelfsema et al., 1997) and, thus, yield a largely consistent picture of cortical dynamics across multiple species.

‖To whom correspondence should be addressed (e-mail: bard@math.pitt.edu [G. B. E.], dk@physics.ucsd.edu [D. K.]).

Evidence for Common Themes in Wave Dynamics

In all vertebrates studied to date, the temporal frequencies of stimulus-driven oscillations are in the range between 10 and 100 Hz, e.g., ~40 Hz in cat visual areas (Gray, 1994). Invertebrates tend to exhibit lower temporal frequencies, e.g., ~1 Hz in the central olfactory system of terrestrial mollusks (Gelperin and Tank, 1990), as well as lower propagation speeds for the waves (Bullock and Horridge, 1965). It is unlikely that the exact value of the frequency is relevant for many aspects of spatial pattern formation. Further, since the wavelength for the pattern is set by the ratio of the propagation speed in the nervous tissue to the frequency of the oscillation, the wavelength for both vertebrates and invertebrates tends to be in the range of 1–10 mm.

The experimental evidence for electrical waves in awake and aroused vertebrate preparations, as well as semiintact and active invertebrate preparations, is consistent with a number of themes (Table 1). (1) The total phase shift is always less than 2π radians (i.e., the spatial extent of the wave is less than one wavelength). Thus, the observed pattern of variation in peak amplitude varies less than one full cycle over areas that span from less than one millimeter (mollusks) to many centimeters (mammals). In addition, the range of the direct interactions (i.e., the combined axonal and dendritic arborization length for monosynaptic connections between cells) are typically less than the spatial extent of the wave. (2) Sensory stimulation may produce a switch in oscillatory dynamics from waves to synchrony, but not the reverse, for sensory systems that oscillate in the absence of stimulation. (3) Whenever there is a switch in electrical output caused by the onset of sensory stimulation, the change is from a lower temporal frequency of oscillations, or from no oscillations, to a higher frequency. Lastly, we note that in motor areas, as opposed to sensory cortices, the effect of sensory stimulation on the form of network oscillations appears less systematic at present (Ahissar and Vaadia, 1990; Murthy and Fetz, 1992; Sanes and Donoghue, 1993).

Theoretical Considerations for Networks of Oscillators

Traveling waves of oscillatory activity take on a number of forms. The simplest pattern is that of a plane wave, in which the membrane voltage of neurons at different locations, denoted $V(x,t)$, is essentially one-dimensional. The amplitude of the wave is a periodic function of time

Table 1. Traveling Waves in Awake Animals

System	Frequency (in Hz)	"Band"	Interstimulus Activity	Stimulus Activity	Phase Gradient Across Area (in Radians)
Molluscan olfactory procerbral lobe (Delaney et al., 1994)	1	—	Wave —	— Synchrony	$\approx\pi$ —
Turtle olfactory cortex (Lam et al., 2000)	12	—	—	Wave	$\sim 3\pi/2$
Rabbit olfactory cortex (Freeman, 1978)	50	γ	—	Wave	$\sim\pi/2$
Turtle visual cortex (Prechtl et al., 1997)	3 20	— γ	Wave —	Wave Wave	$\approx\pi/2$ $\approx\pi$ (plane) 2π (rotating)
Cat visuomotor cortex (Roelfsema et al., 1997)	10 20–40	α γ	Wave —	— Synchrony	$\approx\pi/2$ —
Dog cortex (Lopes da Silva and Storm van Leeuwen, 1978)	8–12	α	Wave	—	$\approx\pi/2$
Human thalamus/cortex (Ribary et al., 1991)	40	γ	Wave	Wave	$\sim\pi$

and space, that is,

$$V(x,t) \propto \sin\left[2\pi\left(\nu t - \frac{\nu}{c}x\right)\right]$$

where ν is the frequency of the oscillator, c is the speed of the wave, and c/ν is the wavelength. Additional patterns occur in two dimensions, the most common of which are target waves, which look like expanding bull's-eyes, and rotating or spiral waves.

Traveling electrical waves may nominally appear from one of three distinct mechanisms. (1) Apparent wave motion may originate when a single neuronal oscillator (i.e., a pacemaker) directly excites neighboring regions of cortex through a progression of increasing time delays (Figure 1a). The wave motion is fictive, much like the lights on a marquee. An example is the wave of current discharge along the length of the electric eel (Bullock and Heiligenberg, 1987). (2) True wave motion may originate from a single neuronal oscillator whose output propagates along a chain of neurons or, equivalently, through serially linked groups of neurons. In this case, wave motion is dependent on the transmission of excitation between neurons (Figure 1b). Examples are waves in the nerve net of coelenterates (Bullock and Horridge, 1965) and possibly low-frequency (i.e., < 1 Hz) waves in neocortex (Sanchez-Vives and McCormick, 2000). (3) The final mechanism involves a network of coupled neuronal oscillators, in which all of the neurons can produce rhythmic output on their own. Thus, wave propagation does not rely on a single pacemaker. Rather, the wave motion originates as stable differences in the phase of the rhythmic output among all of the neuronal oscillators in the network (Figure 1c). The dynamics and functional role of such waves are the focus of our analysis.

The dynamics of individual neurons is governed by a multiplicity of state variables, including membrane voltage, channel activation parameters, and intracellular ion concentrations. When the spiking output of a cell is periodic, or even approximately so, the underlying dynamics may be described by a single variable known as the phase, denoted $\psi(t)$ (Figure 2a). The value of $\psi(t)$ varies over 2π radians as the output of the neuronal oscillator progresses from rest to depolarization to spike generation to repolarization and around again over the course of one period.

Under a variety of conditions, the behavior of networks of neurons with largely oscillatory output may be approximated by a system of equations that govern the phases of each of the oscillators. In this limit, the theory of coupled phase oscillators, which has found broad application to biological, chemical and physical phenomena (Kuramoto, 1984), provides a framework to model experimentally observed oscillations and waves. The strict validity of this approach rests on two assumptions. First, each neuron or group of neurons in the network must be intrinsically oscillatory. Second, the interactions among the neurons, or groups of neurons that comprise an oscillator unit, must be weak. Thus, the activity of one oscillator can affect the timing of another oscillator but cannot distort the form of the oscillators limit cycle, which includes the shape of the action potential (Kuramoto, 1984; Kopell and Ermentrout, 1986). A strength of this theoretical approach is that the phase description can be deduced directly from the underlying biophysics of any neuron for which the ionic basis of the action potential has been deduced (Van Vreeswijk et al., 1994; Hansel et al., 1995).

The phase description provides a means to calculate and understand how the detailed description of the synaptic interactions among neurons can effect their relative timing and, thus, lead to the formation of spatially and temporally patterned electrical output. The essential aspect of the phase description is to calculate the effective interaction, denoted $\Gamma(\psi_i - \psi_j)$, between the phase of the neuronal oscillator at location "*i*" and that at location "*j*." This procedure is described in detail in the Tutorial for the case of a cortical motor neuron that makes excitatory synaptic connections (Figure 2), and the theoretical results are explicitly compared with the data of Reyes and Fetz (1993) (Figure 2b). A strength of this procedure is that the phase differences in neuronal out-

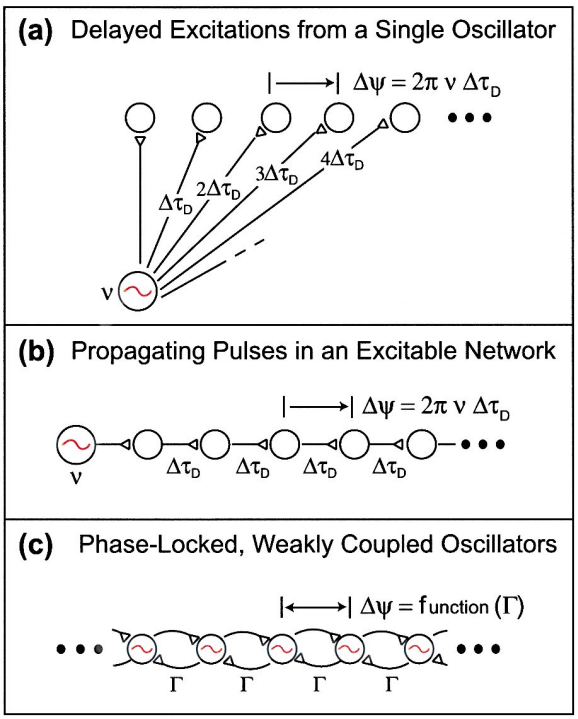

Figure 1. Cartoon of Different Architectures for the Appearance of Phase Differences, $\Delta\psi$, along Cortex

Open circles indicate excitable but not necessarily oscillatory neurons or neuronal tissue, while circles with $\sim$ indicate local oscillators with frequency ν. For simplicity, only one-dimensional models are shown.

(a) A model where the wave motion is fictitious and results from a single oscillator that drives adjacent regions of cortex through increasing time delays of τ_D.

(b) A model where wave motion originates from the transmission of periodic signals along a network of cortical neurons. The propagation delay between neurons is τ_D.

(c) A model where wave motion originates as stable differences in phase among neuronal oscillators that form a network with nearest neighbor coupling, parameterized by Γ (see Tutorial). The value of the phase shift depends on details of the neuronal activation, the isolated frequency, and the interactions. Figure adapted from Prechtl et al. (2000).

put that are calculated for particular network architecture, with biophysically based models for the neurons and their synapses, may be compared directly with the time lag, or relative phase, measured between the electrical signals at two locations in cortex. Typically, such measurements are presented in the form of two-point correlations or spectral coherence.

Tutorial: Phase Reduction for Networks of Weakly Coupled Oscillators

We consider how the biophysical properties of neurons and their synaptic connections are used to determine the dynamics of neuronal activity in the context of the phase oscillator approximation. This limit strictly applies when the interactions among the oscillators are weak, so that the output of one oscillator does not distort the shape of the limit cycle, or action potential, of another. The results of numerical simulations suggest that this approach is useful away from ideal conditions (Grannan et al., 1993; Hansel et al., 1995).

The dynamics of the network is governed by a set of equations that describe the relative phases of the neuronal oscillators at all locations. These equations depend solely on the phase, $\psi(t)$, of each oscillator and only on pairwise interactions. The phase of the oscillator at location "*i*" satisfies

$$\frac{d\psi_i(t)}{dt} = 2\pi\nu + \sum_j \Gamma(\psi_i - \psi_j). \quad (1)$$

The function $\Gamma(\psi_i - \psi_j)$ describes the interaction among the phases of the pair of oscillators at locations *i* and *j*. The sum is only over pairs that form direct connections and, thus, implicitly defines the architecture of the network. The interaction function is periodic [i.e., $\Gamma(\psi_i - \psi_j) = \Gamma(\psi_i - \psi_j + 2\pi)$]. The parameter ν is the frequency of the isolated, or noninteracting oscillator (i.e., Equation 1 with $\Gamma = 0$). For simplicity, we neglected the contribution from noise sources and, further, took the frequency and interaction to be the same for all neurons. In general, the latter parameters differ for different cells [i.e., $\nu \leftarrow \nu_i$ and $\Gamma(\psi_i - \psi_j) \leftarrow \Gamma_{ij}(\psi_i - \psi_j)$].

Two terms, both of which depend on the state variables that underlie the cellular biophysics, appear in the calculation of $\Gamma(\psi_i - \psi_j)$. The first term, denoted by the vector $\vec{Z}(\psi_i)$, delineates the sensitivity of the phase of the postsynaptic neuron to external perturbations to any of its state variables. Each component of $\vec{Z}(\psi_i)$ corresponds to a different state variable, such as voltage, the channel activation parameters, and ion messenger concentration. The form of the sensitivity function, $\vec{Z}(\psi_i)$, may be formally obtained for specific computational models (Figure 2b). The second term, denoted $\vec{P}(\psi_i, \psi_j)$, models how activity in a presynaptic cell, with phase ψ_j, perturbs the state variables of the postsynaptic cell. In analogy to $\vec{Z}(\psi_i)$ each component of $\vec{P}(\psi_i, \psi_j)$ corresponds to perturbation to a different state variable. Of particular interest, the perturbation may result from synaptic input from neighboring presynaptic cells.

The relative phase between two oscillators is assumed to change slowly on the timescale of one period. In this limit, the interaction is found by averaging the product $\vec{Z}(\psi_i, \psi_j) \cdot \vec{P}(\psi_i, \psi_j)$ over one period of oscillation (Kuramoto, 1984) (i.e., over $\theta = 2\pi\nu t$), so that

$$\Gamma(\psi_i - \psi_j) = \frac{1}{2\pi}\int_{-\pi}^{\pi} d\theta\, \vec{Z}(\psi_i + \theta) \cdot \vec{P}(\psi_i + \theta, \psi_j + \theta). \quad (2)$$

To the extent that the perturbation affects only the voltage of the postsynaptic cell, only one component of $\vec{P}(\psi_i, \psi_j)$ is nonzero. We denote this component by the scalar function $P(\psi_i, \psi_j)$. The product $\vec{Z}(\psi_i) \cdot \vec{P}(\psi_i, \psi_j)$ thus depends only on the voltage component of the sensitivity function $\vec{Z}(\psi_i)$ which we denote by the scalar function $Z(\psi_i)$. Thus, the vector product $\vec{Z}(\psi_i) \cdot \vec{P}(\psi_i, \psi_j)$ reduces to the scalar product $Z(\psi_i)P(\psi_i,\psi_j)$.

The voltage dependence of $Z(\psi_i)$ may be determined experimentally with intracellular recording techniques (Reyes and Fetz, 1993). In particular, one injects small pulses of current at all possible phases of the interspike interval and records the shift in instantaneous frequency, $\Delta\nu$, as well as the corresponding change in voltage, denoted ΔV, as a function of ψ. The experimentally determined form of the phase sensitivity is given by

$$Z(\psi) \equiv \frac{\partial\psi}{\partial V} = \frac{2\pi}{\nu}\frac{\Delta\nu}{\Delta V}$$

(Figure 2b). For the case of motor neurons, the match between the values found from a calculation for model of the motor neuron and those observed in vivo is excellent (cf. solid line and closed triangles in Figure 2b). Note that while $Z(\psi)$ is solely positive in this example, in general $Z(\psi)$ can attain both negative and positive values.

For the case of an interaction that is mediated by a chemical synapse, the perturbation term, $P(\psi_i,\psi_j)$, factors as the product of a function of the phase of the postsynaptic cell, ψ_i, times a function of the phase of the presynaptic cell, ψ_j. In particular, the postsynaptic current depends on the release of neurotransmitter by the presynaptic neuron, which is described by a synaptic activation function, denoted $S(V,t)$ (Figure 2c). Further, the current varies in direct proportion to the ionic driving force, which is mediated by the postsynaptic cell.

The above arguments allow us to write the perturbation term for an interaction that is mediated by a chemical synapse as

$$P(\psi_i, \psi_j) = \frac{\bar{g}_{syn}}{C} S(\psi_j)[E_{syn} - V(\psi_i)]$$

where $\bar{g}_{syn}$ is the maximum synaptic conductance, C is the capaci-

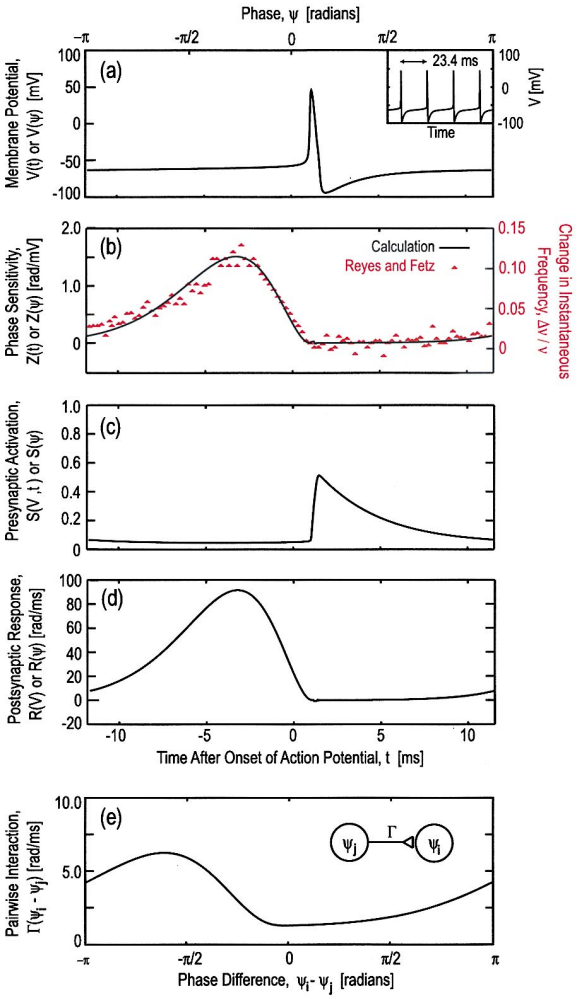

Figure 2. Illustration of the Derivation of the Pair-wise Interaction in the Phase Oscillator Approach (See Tutorial)

(a) A single cycle of the output from a model of a motor neuron. Note the equivalence of the time, denoted t, and the phase, denoted ψ, where $\psi = 2\pi\nu t$ with $\nu^{-1} = 23.38$ ms. The dynamics are described by the circuit equation $CdV/dt = I - g_{Na}m^3h(V - E_{Na}) - g_Kn^4(V - E_K) - g_l(V - E_l) - g_{Ca}m_{l,\infty}(V - E_{Ca}) - g_{ahp}([Ca^{2+}]/([Ca^{2+}] + K_d))(V - E_K)$, and the kinetic equations $dm/dt = a_m(V)(1 - m) - b_m(V)m$, $dn/dt = a_n(V)(1 - n) - b_n(V)n$, $dh/dt = a_h(V)(1 - h) - b_h(V)h$, $d[Ca^{2+}]/dt = -0.002\, I_{Ca} - [Ca^{2+}]/80$, with $m_{l,\infty}(V) = 1/(1 + \exp[-\{V + 25\}/2.5])$, $a_m(V) = 0.32(54 + V)/(1 - \exp[-\{V + 54\}/4])$, $b_m(V) = 0.28(V + 27)/(\exp[\{V + 27\}/5] - 1)$, $a_h(V) = 0.128\exp(-[50 + V]/18)$, $b_h(V) = 4/(1 + \exp[-\{V + 27\}/5])$, $a_n(V) = 0.032(V + 52)/(1 - \exp[-\{V + 52\}/5])$, and $b_n(V) = 0.5\exp(-[57 + V]/40)$. Voltages are expressed in units of mV, $[Ca^{2+}]$ is in units of mM, time is in ms, conductance is in units of mS/cm^2, capacitance is in units of μF/cm^2, and current is in units of μA/cm^2. We chose as parameters: $E_k = -100$, $E_{Na} = 50$, $E_l = -67$, $E_{Ca} = 120$, $g_l = 0.2$, $g_K = 80$, $g_{Na} = 100$, $g_{Ca} = 1$, $g_{ahp} = 1$, $I = 12$, $C = 1$, and $K_d = 0.5$. Insert: succession of action potentials as the neuron produces rhythmic output.

(b) The sensitivity of the postsynaptic neuron, $Z(t)$, to injections of current. The solid line is the result of a calculation, using the model in (a) and the method of Williams and Bowtell (1997). The dots are the measurements of Reyes and Fetz (1993), who injected depolarizing current pulses into the cell.

(c) The time dependence of the activation, $S(\psi)$, induced by a presynaptic action potential. The activation satisfies $dS/dt = 4(1 - S)/(1 + \exp[-\{V + 10\}/10]) - S/2.5$ where V is the voltage of the presynaptic neuron.

(d) The postsynaptic response with where $\bar{g}_{syn} = 1$ and $E_{syn} = 0$.

(e) The pair-wise interaction between the phases of two neuronal oscillators that are connected by an excitatory connection (Equation 3). The calculation makes use of the sensitivity functions for motor neurons (b) with the perturbation given by excitatory synaptic connections (d).

tance of the postsynaptic cell, and E_{syn} is the synaptic reversal potential. In the limit of weak coupling, the magnitude of $\bar{g}_{syn}$ is infinitesimal in comparison with the total conductance of the neuron.

The evaluation of the interaction, $\Gamma(\psi_i - \psi_j)$ (Equation 2), is considerably simplified by the factorization of $P(\psi_i,\psi_j)$ into pre- and postsynaptic terms. The integrand $Z(\psi_i)P(\psi_i,\psi_j)$ can be expressed as the product of the presynaptic activation, $S(\psi_j)$, times a postsynaptic response term, denoted $R(\psi_i)$, that is defined by

$$R(\psi_i) \equiv \frac{\bar{g}_{syn}}{C} Z(\psi_i)[E_{syn} - V(\psi_i)].$$

This function is similar in shape to $Z(\psi_i)$ (cf. Figures 2b and 2d).

The culmination of the above steps allows us to express an interaction that is mediated by a chemical synapse in an intuitive form, that is,

$$\Gamma(\psi_i - \psi_j) = \frac{1}{2\pi}\int_{-\pi}^{\pi} d\theta\, R(\psi_i + \theta)S(\psi_j + \theta) = \frac{1}{2\pi}\int_{-\pi}^{\pi} d\theta\, R(\theta)S[\theta - (\psi_i - \psi_j)]. \quad (3)$$

The resultant interaction corresponds to the correlation between the presynaptic activation and the postsynaptic response. For the case of a motor neuron (Figures 2a–2d), the interaction is strongest when the synaptic input to the postsynaptic cell occurs during the approximately quarter cycle period centered approximately $\pi/2$ radians prior to the output spike (Figure 2e).

Two Oscillator Networks Reveal the Origin of Phase Shifts

The nature of the interaction $\Gamma(\psi_i - \psi_j)$ (Figure 2d and Tutorial) is revealed by considering its effect on a pair of oscillators, which we label "1" and "2" (Figure 3). In general, the neurons are phase locked when the phases of their output evolve with the same time dependence, that is,

$$\frac{d\psi_1(t)}{dt} = \frac{d\psi_2(t)}{dt}$$

case of nonsynchronous phase-locking is antiphase output, for which the two oscillations are one-half cycle apart [i.e., $\psi_1(t) = \psi_2(t) \pm\pi$].

We derived the form for an interaction that is mediated by a chemical synapse (Equations 1 and 2). In the context of a network of two neuronal oscillators (Figure 3a), the part of the interaction that mediates their phase-locking is given by the odd component of $\Gamma(\psi_1 - \psi_2)$, that is,

$$\Gamma_{odd}(\psi_1 - \psi_2) \equiv \Gamma(\psi_1 - \psi_2) - \Gamma(\psi_2 - \psi_1).$$

The odd part always has a zero at phase differences of $\psi_1 - \psi_2 = 0$ and $\psi_1 - \psi_2 = \pm\pi$ and may have zeros at additional phase differences as well (Figure 3b). The zeros correspond to the fixed points of the two oscillator system, whose stability depends on the slope of the odd part of the interaction through the fixed point. The interaction acts as a restoring force for a negative slope and thus the associated fixed point is stable.

For the example of two motor neurons (Figures 2a and 2b) that are coupled by reciprocal, excitatory synapses

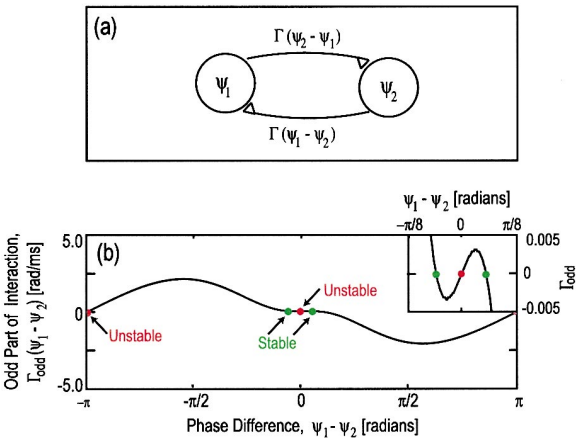

Figure 3. The Odd Part of the Pair-wise Interaction in a Circuit of Two Neuronal Oscillators with Reciprocal Connections

This part controls the phase-locking between the neurons.

(a) Schematic of the architecture.

(b) The odd part of the pair-wise interaction shown in Figure 2e. The insert is an expansion near the origin. Note that the only the points just outside the origin correspond to stable phase differences.

(Figure 2c), the pair-wise interaction (Figure 2d) leads to instability at phase differences of zero and $\pm\pi$ radians but yields stable phase differences of $\psi_1(t) - \psi_2(t) \cong \pm 0.05\pi$ radians (Figure 3b). These phase shifts may mediate waves in a spatially extended network of oscillators. Thus, we have delineated how an effective interaction that was derived directly from biophysical considerations (Equations 1 and 2) can lead to robust phase shifts among neurons.

Phase-locking among a reciprocally connected pair of Hodgkin Huxley neurons, as well as neurons with strong A-type K^+ currents, have been considered (Hansel et al., 1993, 1995; Van Vreeswijk et al., 1994). For the case of neurons that form solely inhibitory synapses with sufficiently slow kinetics, the results from these studies predict that networks with all inhibitory connections should exhibit synchronous phase-locking, a seemingly counterintuitive result. Experimental verification of the theoretical prediction of synchronous phase-locking in networks of neurons with solely inhibitory synaptic connections was observed in a mammalian slice preparation (Whittington et al., 1995; J. Gibson et al., 2000, Soc. Neurosci., abstract).

Phase Coherence Persists in the Presence of Noise

The formalism we discussed so far (Equation 1) excluded sources of variability. We now discuss two such sources that may affect the dynamics of the network. The first source is fast noise, e.g., fluctuations in the phases of each neuronal oscillator that are fast compared to the period of oscillation, ν^{-1}. In general, fast noise will lead to a distribution of phase shifts, $\psi_i(t) - \psi_j(t)$, among neighboring oscillators. The phase shifts are centered around their mean value, such as the nonzero shifts for the stable points calculated above (Figure 3b) or phase differences of zero for synchronous output. The width of the distribution will be proportional to the standard deviation of the noise. At sufficiently high levels of noise, the phase coherence among neighboring oscillators is destroyed (Sompolinsky et al., 1991).

In terms of measurements, fast noise will broaden the observed two-point correlation between the output of neighboring oscillators. Thus, for example, correlations on the timescale of individual action potentials may be averaged out while correlations on the timescale of bursts of action potentials are preserved.

A second source of variability is a distribution in the values of the parameters that underlie the calculation of $\Gamma(\psi_i - \psi_j)$, or a distribution in the values of the isolated frequencies ν_i. For the particular case of a distribution in frequencies, each oscillator can frequency- and phase-lock with a relative phase shift that depends on the difference between its isolated frequency and that achieved by the phase-locked network of oscillators. The spatial organization of phase shifts will reflect the spatial distribution of oscillators with different values of isolated frequencies. Importantly, when the oscillators are arranged in order of increasing isolated frequency, the network will exhibit waves that propagate from neurons with higher isolated frequency to neurons with lower frequency as a result of the imposed spatial gradient; we will illustrate this point by two examples (Figures 3 and 5). With respect to the general issue of an inhomogeneous distribution of neuronal parameters, it has been shown that networks can still achieve stable, coherent output (White et al., 1998; Golomb and Hansel, 2000; Neltner et al., 2000).

Theory versus Experiment in Spatially Extended Networks

The main theoretical challenge is to understand under what conditions one expects to observe traveling waves, as opposed to synchronous oscillations, in nervous systems. Three effects dominate the behavior of coupled networks of oscillators and the nature of their output: (1) the pull toward and push away from synchrony, as mediated by pair-wise interactions between coupled neuronal oscillators, $\Gamma(\psi_i - \psi_j)$ (Figures 2d and 3b); (2) the topology of the connections, as defined by the architecture of the network; and (3) possible heterogeneity among the properties of oscillators that comprise the network.

One-Dimensional Networks: Plane Waves and Synchrony in Nonmammalian Cortices

One or more of the above mechanisms can easily produce spatial phase gradients that approximate plane waves and have found use in the modeling and analysis of central pattern generators responsible for locomotion in invertebrates (Cohen et al., 1992; Friesen and Pearce, 1993; Marder and Calabrese, 1996). For example, consider an architecture in which neurons are arranged as a chain (i.e., in a line with connections only between nearest neighbors). Heterogeneity in the form of a gradient in intrinsic frequencies of the individual neurons, e.g., $\nu = \nu_o + (\partial\nu/\partial x)x$, where ν_o and the frequency gradient $\partial\nu/\partial x$ are constants and x is the distance along the chain of oscillators, will induce a gradient in the relative phases of the coupled system. The concomitant plane waves will propagate opposite to the direction of the gradient. Alternatively, systematic phase differences between oscillators that organize into a traveling wave may originate from connections that are spatially asymmetric

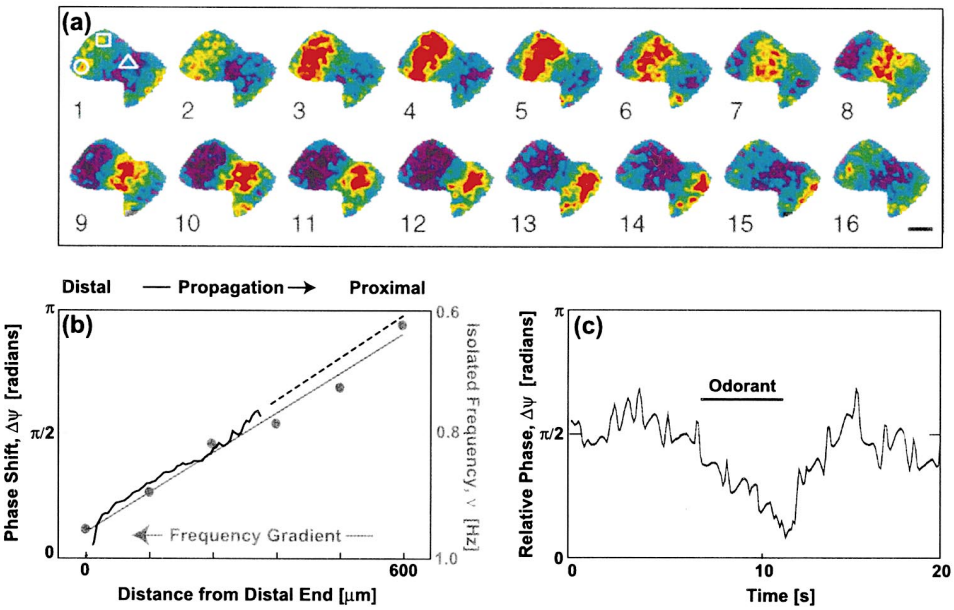

Figure 4. Wave Motion in One Dimension, Using the Central Olfactory Lobe of the Mollusk *Limax* as an Example

(a) Successive images of the membrane potential in the olfactory lobe over the course of one cycle. Note the band of depolarization (pseudocolored red) that propagates distal to proximal, followed by hyperpolarization. The timescale is 112 ms/frame and the bar is 100 μm. Adapted from Kleinfeld et al. (1994).

(b) Dark line: the phase shift of the accompanying traveling measured in the intact animal; solid curve adapted from Kleinfeld et al. (1994) and broken line based on unpublished data of K. R. Delaney and D. K. Light line: the measured frequency of oscillation for intrinsic oscillators in successive 125 μm slices (black curve) cut normal to the distal–proximal axis; adapted from Ermentrout et al. (1998).

(c) Phase difference across two points on the distal–proximal axis, similar to the locations of the square and triangle in frame 1 of (a), before, during, and after odor presentation. Note the transition from waves ($\Delta\psi \approx \pi/2$ radians) to near synchronous activity ($\Delta\psi \approx 0$). Panel adapted from Gervais et al. (1996).

(Kopell and Ermentrout, 1986). More generally, oscillators that are coupled with short-range synchronizing connections, along with a relatively sparse set of long-range desynchronizing interactions that encourage antiphasic behavior, can organize as a traveling wave (Ermentrout and Kopell, 1994). The converse of the last example also holds; a few properly placed long-range synchronizing interactions can overcome short-range phase gradients and force the network toward synchrony.

Models for wave motion along chains of oscillators provide a means to understand the special case of plane waves in two dimensions. We consider the case of electrical waves in the olfactory lobe of the terrestrial mollusk *Limax*. This animal utilizes olfaction as its primary sense and has a central olfactory organ whose cell count and local circuitry is reminiscent of the vertebrate olfactory bulb (Chase and Tolloczko, 1993). Intracellular and optical imaging studies revealed the presence of periodically driven plane waves of electrical activity along the lobe in the absence of sensory stimulation (Delaney et al., 1994; Kawahara et al., 1997; Nikitin and Balaban, 1999). These waves appear as a band of depolarization that starts at the distal end of the lobe and travels along the axis of the preparation (Figure 4a). The measured phase gradient is nearly linear (Kleinfeld et al., 1994) (dark curve, Figure 4b). Interestingly, the application of an odor stimulus leads to a transient switch from the state with waves to one in which the output from neurons across the lobe is nearly synchronous (Figure 4c) (Delaney et al., 1994).

As a means to determine if a spatial gradient of natural frequencies in the underlying neurons can account for the traveling waves in the molluskan olfactory lobe, individual slices of the lobe were prepared at successively different distances from the distal end of the lobe (Figure 4a). The frequency of oscillations for each isolated slice was found to increase as a function of distance, with the highest frequency observed in slices prepared near the distal end (Kleinfeld et al., 1994; Ermentrout et al., 1998) (light curve, Figure 4b). Thus, propagation initiates in the part of the lobe with the highest intrinsic frequency, consistent with theoretical expectations. Further, the linearity of the observed phase shifts (dark curve, Figure 4b) is consistent with the predictions from a model based on a linear gradient of natural frequencies among coupled oscillators (Ermentrout et al., 1998).

The switch toward synchrony observed in response to odor in the molluskan olfactory network (Figure 4c) may be understood in terms of a network that, in addition to short-range connections, contains a sparse distribution of long-range connections. In this model, the long-range connections must mediate pair-wise interactions that tend to synchronize neuronal output, and, further, they must be gated by an external mechanism, such an as overall increase in neuronal activity that accompanies the onset of stimulation (Ermentrout et al., 1998). In support of this model, anatomical evidence shows that long-range connections occur in the molluskan olfactory lobe (Watanabe et al., 1998) and that these connections are activated by increased excitation of the target neurons

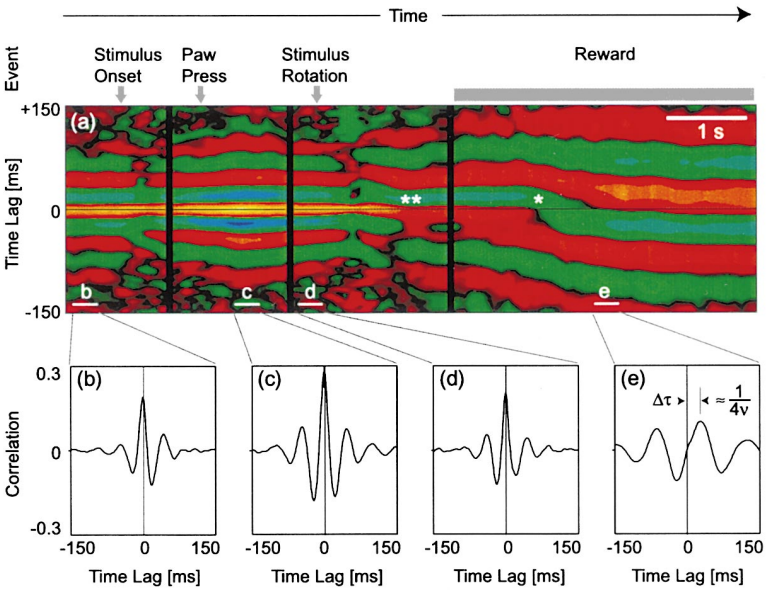

Figure 5. Evidence for Traveling Waves along the Visuomotor Pathway in Cats.

Local field potentials were measured in two sites across parietal association cortex, area 7 and the lateral aspect of area 5, during a forced choice discrimination task in which the animal was trained to respond to a change in the orientation of a grating. The task can be divided into separate epochs: (1) the onset of the grating stimulus, (2) pressing a level once the grating is perceived, (3) releasing the lever in response to a rotation of the grating, and (4) a period of food reward before the grating reappears to start a new trial.

(a) Two-point correlations in a sliding 0.5 s temporal window were computed from local field potential measurements in parietal area 7 and the lateral subdivision of area 5 throughout the behavioral epoch. The colors label the sign (yellow/red = "+" and blue/green = "−") of the correlation. Note the presence of a phase shift, **, that originates soon after the cat makes a behavioral choice, with $\Delta\psi \approx \pi/2$ radians. A further flip of π radians (*) occurs during the reward period.

(b–e) Graphs of the two-point correlations taken from 0.5 s intervals, as indicated by the line segments in (a). Figure adapted from Roelfsema et al. (1997).

by odor stimuli (Inoue et al., 2000). An analogous mechanism is posited to mediate synchrony across oscillators in neocortex (Whittington et al., 1997), although the relatively slow propagation speed along such connections may preclude their role in synchronization (Bringuier et al., 1999).

Traveling Waves in Mammalian Cortex

The pioneering studies of Lily and Petsche and others (reviewed by Hughes, 1995) suggested that sensory stimulation led to traveling electrical waves in the cortex of cat. Nonetheless, a preponderance of experimental data, typically in the form of two-point correlations between the spiking output of neurons, has documented the occurrence of synchronous output, as opposed to the production of traveling waves (Gray, 1994). It is important to recall that much of this data was obtained with anesthetized animals, including cat, monkey, and most recently mouse (G. Nase et al., 2000, Soc. Neurosci., abstract), and that most experimental studies only addressed responses that occurred close to or during the period of visual stimulation. In contrast, a study by Roelfsema et al. (1997) considered the electrical dynamics along the cat visual system in awake animals that performed a forced discrimination task, in which the animal was trained to respond to changes in the orientation of a bar. The observed correlations of electrical activity across areas 5 and 7 of parietal visual cortex show clear timing differences, which suggests that traveling waves are present during the periods of behavioral choice and reward (Figures 5a and 5e) with $\Delta\psi = 2\,\pi\nu\Delta\tau \approx \pi/2$ (Figure 5e). Cantrawise, synchrony is present while the animal attends to a single visual stimulus (Figures 5a–5d).

The measurements of Roelfsema et al. (1997) further show a rapid switch between synchronous electrical activity and phase shifts of approximately $\pi/2$ radians (double asterisks in Figure 5a), as well as switching among phase shifts (single asterisk in Figure 5a) (P. Roelfsema, personal communication). Unlike the case for mollusks, the switch from phase gradients to synchrony is eventually accompanied by a substantial increase in frequency. However, similar to the case for mollusks (Figure 5c), phase shifts are the basal response and the anticipation or onset of a behavioral trial induces a switch to synchrony. It is presently unknown if the phase shifts in mammalian cortex are part of rotating as opposed to plane waves. However, past experiments on phase shifts within cat primary visual cortex (Konig et al., 1995) and ongoing experiments in the visuomotor system of monkey (Munk et al., 1999; M. Munk et al., 2000, Soc. Neurosci., abstract) show that a multitude of phase relations are present through visual areas; this includes anticorrelation and dynamic phase shifts during the performance of the visuomotor task (Munk et al., 1999). It will be interesting to learn if components of these patterns are part of plane or rotating waves, as occurs in turtle (Prechtl et al., 1997). In particular, the frequency of the basal wave motion suggests that they are part of the α rhythm (Roelfsema et al., 1997), which exhibits phase shifts across cortex (Lopes da Silva and Storm van Leeuwen, 1978; Arieli et al., 1995; see also Jones et al., 2000).

The switch toward synchrony observed in response to the appearance of an oriented bar (Roelfsema et al., 1997), as well as changes in the extent of synchrony as a function of the relative orientation of two bars in the visual field (Gray et al., 1990), may be understood in terms of activity-dependent changes in the interactions between the underlying neuronal oscillators. The pairwise interaction between the phases of neuronal oscillators that are arranged in specific architectures may be

determined similarly to that for single cells (see Tutorial). The analysis of the interaction between two model networks that approximate cortical hypercolumns shows that the magnitude and phase shifts of the interaction depend on the product of the activity of the pre- and postsynaptic neuronal oscillators (Grannan et al., 1993). These changes in the synchronization properties of the effective interaction are solely a consequence of the underlying architecture and dynamics in a network with static synaptic strengths, as opposed, e.g., to biophysical changes in synaptic strength. They originate from changes in the relative activation of neuronal populations with different orientation preferences (Schuster and Wagner, 1990; Grannan et al., 1993). This mechanism provides a means by which changes in visual stimulus may mediate the extent of synchrony across neurons in visual cortex (Sompolinsky et al., 1990).

A Test of the Phase Model in Visual Cortex

The case of stimulus-induced oscillations in the mammalian visual cortex is a potential test bed to probe the validity of the phase-coupled oscillator approach in mammalian cortex (Sompolinsky et al., 1991). We exploit the observation that the frequency of the cortical oscillation is a slowly varying function of the different features of a drifting stimulus, such as speed or temporal frequency (Eckhorn et al., 1988; Gray et al., 1990; Friedman-Hill et al., 2000) and possibly contrast (J. A. Movshon, 1993, Soc. Neurosci., abstract). We consider a situation where separate stimuli, in this case moving bars, are simultaneously presented to nonoverlapping classical receptive fields. For the case of moving bars that are aligned with the same orientation, previous results have shown that the neuronal output from the corresponding areas of primary visual cortex will clearly oscillate in synchrony (Gray et al., 1989).

We consider the hypothetical case in which the bars have equal orientation but, for the sake of argument, may differ in speed (Figure 6). The timing of the presentation is arranged so that both stimuli activate their respective receptive fields at the same time, even if one bar moves faster than the other does. For the case with bars with unequal speed, we denote the frequency of oscillations induced by the faster bar alone as ν_f and the frequency of oscillations induced by slower bar alone as ν_s. We predict that the simultaneous presentation of the two stimuli will lead to phase-locking among the neuronal oscillators with a frequency intermediate to that of ν_f and ν_s (Figures 6b and 6c). Critically, similar to the case of a spatial gradient of phases (Figure 4c), the difference in intrinsic frequencies will produce a phase shift between the two neuronal oscillators that is a function of $\nu_f - \nu_s$ (Kuramoto, 1984), that is,

$$\Delta\psi \equiv \psi_f - \psi_s = \Gamma_{odd}^{-1}\left(\frac{\nu_f - \nu_s}{\Gamma_o}\right) \qquad (4)$$

where Γ_o is a constant that scales the magnitude of the phase interaction; $\Gamma_o \approx 4\pi(g_{syn}/C)|(\Delta\nu/\nu)/(\Delta V/V)|$ in the notation of Equation 3. This phase shift (Equation 4) will be apparent in the measured correlation function between spike activity from the two areas and is analogous to the case of continuous phase shifts in a chain of oscillators with a spatial gradient of intrinsic frequencies (Figure 4b). Lastly, for sufficiently large frequency differences, the neuronal oscillators will no longer frequency lock. Although an experiment of this type has not been performed, the feasibility of such an experiment is suggested by measurements of the variable phase shift between rhythmic behaviors and the hippocampal τ rhythm in rat (Semba and Komisaruk, 1978; Macrides et al., 1982).

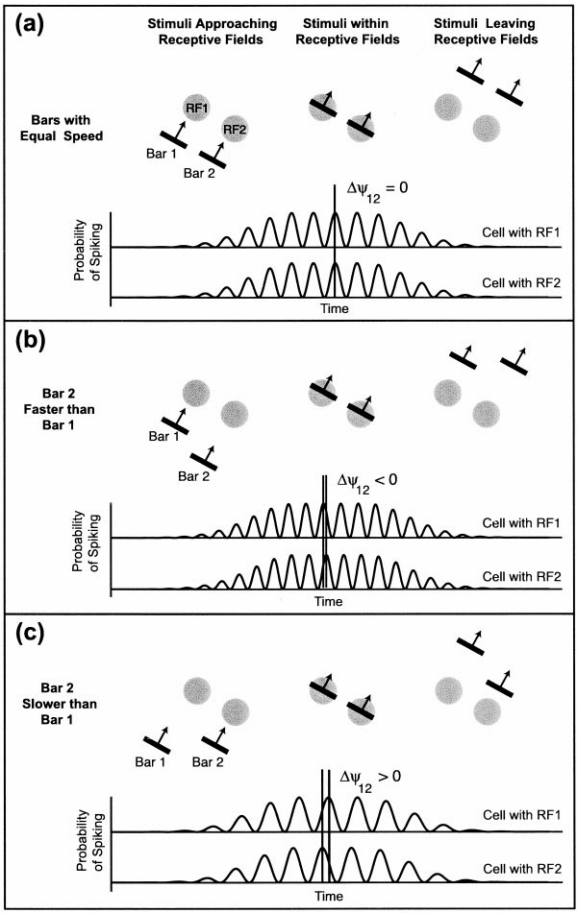

Figure 6. Schematic of a Proposed Test of the Phase Description in Terms of Excitation of Units in Primary Visual Cortex with Separate Receptive Fields

The receptive fields are denoted by the filled gray circles, the stimuli are the moving bars, and the oscillatory response of units in each region is denoted by the periodically varying probability in spike rate. Note that units in the different areas are assumed to frequency-lock with a phase difference, $\Delta\psi$, that depends on their intrinsic frequencies (i.e., the frequencies observed with the presence of only bar 1 or bar 2; see Equation 4 for details).

(a) Bars of equal orientation and equal speed excite neurons with nonoverlapping classical receptive fields. The probability of spiking of the units are, on average, frequency locked and synchronous (i.e., $\Delta\psi_{12} = 0$), as observed in experiment (Gray et al., 1989).

(b) Bars of equal orientation and unequal speed excite units with nonoverlapping classical receptive fields. The probability of spiking of the units are, on average, frequency locked. The phase of the units that respond to the faster bar leads (i.e., $\Delta\psi_{12} > 0$).

(c) Bars of equal orientation and unequal speed excite units with nonoverlapping classical receptive fields. The probability of spiking of the units are, on average, frequency locked. The phase of the units that respond to the slower bar lags (i.e., $\Delta\psi_{12} < 0$).

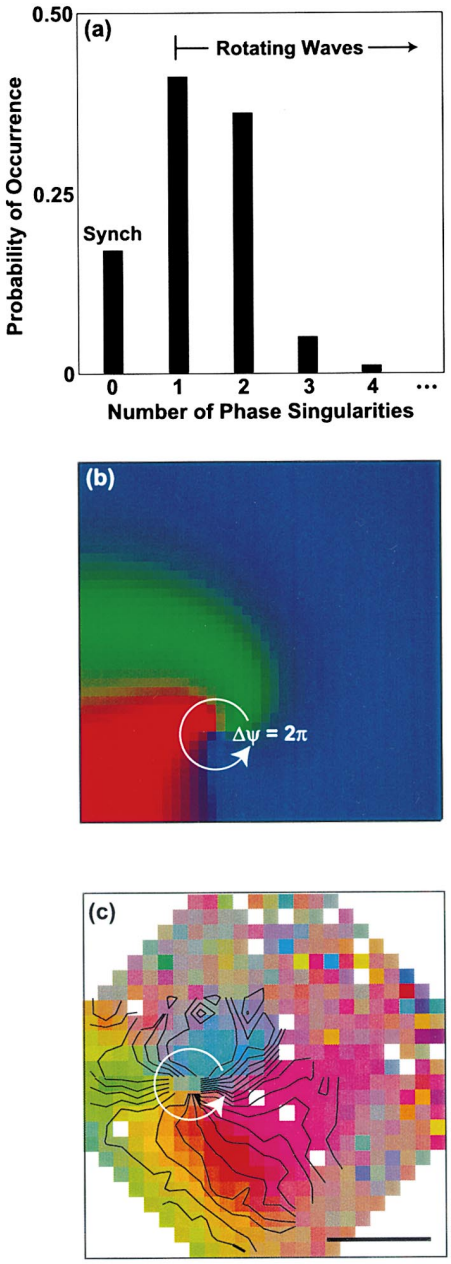

Figure 7. Rotating Waves in Two-Dimensional Networks

(a and b) Aspects of theoretically predicted wave motion for a network of model neurons with isotropic, short-range connections (Equation 1). An array of 40 by 40 phase oscillators, with each site described by a phase, $\psi_{xy}(t)$, were coupled with their nearest neighbors, where the interactions are identical in form for all pairs and are given by $\Gamma[\psi] = A_1 \sin(\psi + \alpha_1) + A_2 \sin(2\psi + \alpha_2)$. We chose the parameters $A_1 = 1.00$, $A_2 = 0.50$, $\alpha_1 = 0.67\pi$ radians, and $\alpha_2 = 0.41\pi$ radians (i.e., the values for $\Delta\theta_0 = \pi/8$ radians in Figure 3 of Grannan et al. [1993]). (a) shows a histogram of the relative number of initial conditions that led to synchronous electrical activity, where all neurons fire together, as opposed to patterned activity with one or more rotating waves as the stable configuration. (b) is a plot, in two spatial dimensions (x, y), of the relative phase of the steady-state oscillatory output at each site, $\psi_{xy}(t)$, for the model network. We chose an initial condition that led to patterned output with one rotating waves; the phase of neuronal firing changes by 2π as one circles the center, or singular point, of the rotating wave. Each phase is labeled by a different color.

(c) Optical image of a rotating wave in dorsal cortex of turtle, the solely visual area for this animal, during a visual stimulus that consisted of a slowly looming ball. The underlying oscillation had a frequency of 18 Hz. We plot only the relative phase (i.e., the complex demodulate of the electrical activity during a 200 ms window that contained the rotating wave). The amplitude of the demodulate is labeled by the saturation level of the color and the phase is labeled by the hue; the accompanying contour lines of constant phase are drawn every $\pi/12$ radians. Note the circular phase gradient; this is the signature of a rotating wave. The scale bar is 1 mm. Panel adapted from Prechtl et al. (1997).

Two-Dimensional Networks: Rotating Waves and Synchrony

The theory of patterned electrical output for networks of coupled oscillators in two-dimensional networks is presently incomplete. On the one hand, the problem is simple in that the onset of spatial phase gradients, as well as more complex phenomena, can occur in networks with identical oscillators and symmetric coupling solely to nearest neighbors. Thus, unlike the case for waves in one-dimensional networks, two-dimensional networks can support persistent patterns of electrical activity in the absence of asymmetric connections or an inhomogeneous distribution of parameters (Figures 1 and 4). On the other hand, the problem of patterned electrical output in two-dimensional networks is difficult as a multiplicity of output patterns may occur in the same network. The details of these patterns depend on the underlying cellular mechanism for the oscillations, the nature of the synaptic connections between the neurons, the boundary conditions for the network, and the initial pattern of electrical activation. Nonetheless, such generic features as rotating electrical waves and synchronous output emerge from studies on coupled neuronal oscillators (Paullet and Ermentrout, 1994).

To illustrate the spontaneous appearance of waves in a two-dimensional network, we consider the model for phase oscillators, $\psi_i(t)$ (Equation 1), on a 40 $\times$ 40 lattice, so that each index "i" corresponds to a location (x, y). We couple the neurons only to their nearest neighbors and use an interaction function, $\Gamma(\psi_{xy} - \psi_{x'y'})$, derived from a model for interacting cortical hypercolumns (Grannan et al., 1993). This particular interaction function is synchronizing (i.e., an isolated pair of oscillators that are mutually coupled by this interaction will always synchronize the phase of their output). However, while synchrony is one possible state in the two-dimensional coupled lattice, it is not the only possibility. The results from simulations of the model show that the steady-state output patterns are either spatial synchrony or consist of one or more rotating waves (i.e., phase singularities or "pinwheel" centers) (Figure 7a). The presence of a particular pattern depends on the initial state of each oscillator; a single rotating wave is stable for the example of Figure 7b. Each pattern is stable to small changes to the initial state. In some cases, the patterns never reach steady state, so that the centers of rotation drift with time.

Support for the experimental occurrence of rotating waves under normal physiological conditions was provided only recently by imaging measurements of the membrane voltages across neurons in turtle visual dor-

sal cortex (Prechtl et al., 1997). The electrical activity exhibits a low-frequency traveling wave in the absence of stimulation (Table 1). A separate, high-frequency traveling wave appears in response to visual stimulation. This wave clearly rotates for part of the epoch (Figure 7c). Recent, two-point correlation measurements across current sources in cortex revealed that the waves result from a network of underlying cortical oscillators (Prechtl et al., 2000). The interactions responsible for the rotating wave are likely to be mediated by the horizontal cortical connections (Cosans and Ulinski, 1990).

The Computational Role of Traveling Waves

We first consider the potential benefit of oscillations per se. It has been hypothesized (Hopfield, 1995) that oscillating membrane potentials provide a means to heighten the sensitivity of neurons to changes in their inputs. One biophysical mechanism for this is through the periodic deinactivation of the Hodgkin-Huxley Na^+ current. The scale of voltage changes necessary for this process is the difference between the rest potential of the neuron and the onset of inactivation for the Na^+ channel, about 10 mV. This scale is similar to that seen in intracellular recordings from neurons with oscillatory subthreshold activity in Limax (Gelperin and Tank, 1990) and in cat primary visual cortex (Gray and McCormick, 1996). Note that periodic deinactivation renders the neuron largely unresponsive to input while it is transiently hyperpolarized.

A related potential benefit of oscillatory potentials is to shift the spiking output of a neuron toward the peak of the depolarized phase of the oscillations. This occurs since the excitability of neurons is greatest during activating versus inactivating phases of the underlying ionic currents, as shown experimentally (Lampl and Yarom, 1993; Reyes and Fetz, 1993; Mellon and Wheeler, 1999) and in numerical simulations (Diesmann et al., 1999). Thus, largely irrespective of when inputs arrive, the rhythmic output of a neuron appears as bursts of spikes.

We consider two potential computational roles for waves based on their emergence solely as a consequence of oscillations in networks with predominantly short-range synaptic connections. These augment the computational benefit of purely synchronous oscillations discussed above. First, to the extent that periodic deinactivation heightens the sensitivity of neurons to respond to changes in their input, the presence of traveling electrical waves ensures that only part of the sensory field is rendered unresponsive during each period of the oscillations. This is in contrast to the periodic epochs of inattention that may occur in a solely synchronous network.

The second potential computational role follows from the finding that neurons are most sensitive to changes in their input that occur in the one-half period prior to their firing an action potential (Figure 2b). Traveling waves ensure that some fraction of the neurons are maximally sensitive to changes in their input at any given time. As such, traveling waves cause sensory areas to function like a "bar code scanner," so that a fraction of the total sensory field is optimally probed, or attended to, at each instance. The entry of a feature into the sensory field is further hypothesized to lead to synchronous activity. This scheme is reminiscent of Crick's (1984) searchlight hypothesis (see also Ribary et al., 1991).

The "bar code scanner" hypothesis may be experimentally tested by monitoring the sensitivity of a behavioral response as a function of the phase of the underlying oscillation. As a concrete, albeit oversimplified proposal, we consider the case of the visual response in the trained cat. As shown by Roelfsema et al. (1997), the onset of cortical synchronization coincides with the initiation of an experimental trial period. We suggest that the latency to synchronization will systematically vary with the phase of the underlying cortical oscillation relative to the onset time of the trial. The timescale for the differences in latency should be a fraction of the period of the underlying oscillations (i.e., up to 10–15 ms for 40 Hz oscillations and a maximal phase shift of π radians across cortex). With regard to spatial aspects of the latency to synchronization, regions of cortex with different receptive fields but similar phase in their electrical activity are expected to exhibit the same latency. The use of a fixation cue to define the onset of a trial will prove crucial to the proposed experiment.

Lastly, we speculate that traveling electrical waves may serve to label simultaneously perceived features in the stimulus stream with a unique phase. To the extent that different areas of cortex are organized as maps of their respective sensory field, such as the retinotopic organization in visual areas, the presence of waves allows sensory activity at different spatial locations to be tagged with a different temporal phase. Further, the current experimental data shows that electrical waves propagate across neuronal areas with a total variation in phase that is less than 2π (Table 1), even though traveling waves could, in principle, encompass multiple cycles across an area. Thus, sensory activity at different spatial locations is tagged with a unique value of phase. In the context of models of associative neural networks, the addition of phase information may be used as a means to segment and categorize multiple inputs from each other and segment inputs from background (von der Malsberg and Schneider, 1986; Sompolinsky and Tsodyks, 1994; Wang and Terman, 1997).

The Switch from Waves to Synchrony

Subtle changes in the effective interaction between neuronal oscillators can tip the stability of a network from one supporting traveling waves to one supporting only synchrony or near synchrony. One mechanism, discussed in the context of waves in the olfactory system of *Limax* (Figure 4), involves the activation of synchronizing long-range interactions between the phases of neuronal oscillators and was posited to control the switch in the mulluscan olfactory lobe (Ermentrout et al., 1998) (Figure 4b). A second mechanism, discussed in the context of synchrony in the mammalian visual system (Figure 5), involves interactions between the phases of oscillators whose strength is mediated by the pattern of external stimulation (Sompolinsky et al., 1990). A third mechanism involves stimulus-induced changes in the frequency of the oscillators in a network that, in turn, alter the synchronization properties of the network (Whittington et al., 1997; White et al., 1998; J. Gibson et al., 2000, Soc. Neurosci., abstract). One mechanism for this is

when the temporal delays in axonal transmission exceed a fraction of the period of the oscillations, e.g., $\tau_D = (4\nu)^{-1}$ for the case of sinusoidal oscillations, so that synchronizing synaptic inputs switch to antiphasic inputs as ν increases, and vice versa.

The sensitivity of the switch from traveling waves to synchrony, or near synchrony, suggests that the switch may be of great computational utility. Yet the role of this switch is presently a matter of speculation. In this guise, we note that coherent activity among a large number of neurons could aid in the strengthening or weakening of synaptic connections through Hebbian mechanisms. Recent experimental evidence suggests that such plasticity occurs only when pre- and postsynaptic spikes occur within a narrow temporal window (i.e., $\sim$20 ms) and that the sign of the synaptic change depends critically on the relative timing of pre- versus postsynaptic activation (Bell et al., 1997; Markram et al., 1997; Bi and Poo, 1998; Feldman, 2000). Thus, the switch from traveling waves to near synchrony, which occurs only in the presence of stimulation, may further serve to gate synaptic plasticity.

Acknowledgments

This project originated as a joint lecture for the "Methods in Computational Neuroscience" summer school at the Marine Biological Laboratory. We thank A. D. Reyes for kindly supplying his data for Figure 2b, K. R. Delaney for collaborating on measurements that yielded data for Figure 4b, P. R. Roelfsema and W. Singer for kindly supplying the material for Figure 5, A. Gelperin for bibliographic material, B. I. Shraiman for his suggestion of the "bar code scanner" hypothesis, K. Blum, F. F. Ebner, B. Friedman, D. Golomb, N. Kopell, H. Levine, N. C. Spitzer, and R. Wessel for comments on earlier versions of the manuscript, and the anonymous reviewers for constructive criticisms. Supported by the NIMH (G. B. E. and D. K.), the NSF (G. B. E.), and the Whitehall Foundation (D. K.).

References

Ahissar, E., and Vaadia, E. (1990). Oscillatory activity of single units in a somatosensory cortex of an awake monkey and their possible role in texture analysis. Proc. Natl. Acad. Sci. USA *87*, 8935–8939.

Arieli, A., Shoham, D., Hildesheim, R., and Grinvald, A. (1995). Coherent spatiotemporal patterns in ongoing activity revealed by real-time optical imaging coupled with single-unit recording in the cat visual cortex. J. Neurophysiol. *73*, 2072–2093.

Bell, C.C., Han, V.Z., Sugawara, Y., and Grant, K. (1997). Synaptic plasticity in a cerebellum-like structure depends on temporal order. Nature *387*, 278–281.

Bi, G.Q., and Poo, M.-M. (1998). Synaptic modifications in cultured hippocampal neurons: dependence on spike timing, synaptic strength, and postsynaptic cell type. J. Neurosci. *18*, 10464–10472.

Bringuier, V., Chavane, F., Glaeset, L., and Fregnac, Y. (1999). Horizontal propagation of visual activity in the synaptic integration field of area 17 neurons. Science *283*, 695–699.

Bullock, T.H., and Heiligenberg, W. (1987). Electroreception (New York: Wiley).

Bullock, T.H., and Horridge, G.A. (1965). Structure and Function in the Nervous Systems of Invertebrates, Volume 1 (San Francisco: W. H. Freeman).

Castelo-Branco, M., Neuenschwander, S., and Singer, W. (1998). Synchronization of visual responses between the cortex, lateral geniculate nucleus, and retina in the anesthetized cat. J. Neurosci. *18*, 6395–6410.

Chase, R., and Tolloczko, B. (1993). Tracing neural pathways in snail olfaction: from the tip of the tentacles to the brain and beyond. Microsc. Res. Tech. *24*, 214–230.

Cohen, A.H., Ermentrout, G.B., Kiermel, T., Kopell, N., Sigvardt, K.A., and Williams, T.L. (1992). Modeling of intersegmental coordination in the lamprey central pattern generator for motion. Trends Neurosci. *15*, 434–438.

Cosans, C.E., and Ulinski, P.S. (1990). Spatial organization of axons in turtle visual cortex: intralamellar and interlamellar projections. J. Comp. Neurol. *296*, 548–558.

Crick, F. (1984). Function of the thalamic reticular complex: the searchlight hypothesis. Proc. Natl. Acad. Sci. USA *81*, 4586–4590.

Delaney, K.R., Gelperin, A., Fee, M.S., Flores, J.A., Gervais, R., Tank, D.W., and Kleinfeld, D. (1994). Waves and stimulus-modulated dynamics in an oscillating olfactory network. Proc. Natl. Acad. Sci. USA *91*, 669–673.

Diesmann, M., Gewaltig, M.O., and Aertsen, A. (1999). Stable propagation of synchronous spiking in cortical neural networks. Nature *402*, 529–533.

Eckhorn, R., Bauer, R., Jordan, W., Brosch, M., Kruse, W., Munk, M., and Reitboeck, H.J. (1988). Coherent oscillations: a mechanism of feature linking in the visual cortex? Biol. Cybern. *60*, 121–130.

Ermentrout, G.B., and Kopell, N. (1994). Inhibition-produced patterning in chains of coupled nonlinear oscillators. SIAM J. Appl. Math. *54*, 478–509.

Ermentrout, G.B., Flores, J., and Gelperin, A. (1998). Minimal model of oscillations and waves in the Limax olfactory lobe with tests of the model's predictive power. J. Neurophysiol. *79*, 2677–2689.

Feldman, D.E. (2000). Timing-based LTP and LTD at vertical inputs to layer II/III pyramidal cells in rat barrel cortex. Neuron *27*, 45–56.

Freeman, W.J. (1978). Spatial properties of an EEG event in the olfactory bulb and cortex. Electroenceph. Clin. Neurophysiol. *44*, 586–605.

Friedman-Hill, S., Maldonado, P.E., and Gray, C.M. (2000). Dynamics of striate cortical activity in the alert macaque: I. Incidence and stimulus-dependence of gamma-band neuronal oscillations. Cereb. Cortex *10*, 1105–1116.

Friesen, W.O., and Pearce, R.A. (1993). Mechanism of intersegmental coordination in leech locomotion. Semin. Neurosci. *5*, 41–47.

Gelperin, A., and Tank, D.W. (1990). Odour-modulated collective network oscillations of olfactory interneurons in a terrestrial mollusc. Nature *435*, 437–440.

Gervais, R., Kleinfeld, D., Delaney, K.R., and Gelperin, A. (1996). Central and reflexive responses elicited by odor in a terrestrial mollusk. J. Neurophysiol. *76*, 1327–1339.

Golomb, D., and Hansel, D. (2000). The number of synaptic inputs and the synchrony of large, sparse neuronal networks. Neural Comp. *12*, 1095–1139.

Grannan, E.R., Kleinfeld, D., and Sompolinsky, H. (1993). Stimulus dependent synchronization of neuronal assemblies. Neural Comput. *5*, 550–569.

Gray, C.M. (1994). Synchronous oscillations in neuronal systems: mechanisms and functions. J. Comput. Neurosci. *1*, 11–38.

Gray, C.M., and McCormick, D.A. (1996). Chattering cells: superficial pyramidal neurons contributing to the generation of synchronous oscillations in the visual cortex. Science *274*, 109–113.

Gray, C.M., Engel, A.K., Konig, P., and Singer, W. (1989). Stimulus-dependent neuronal oscillations in cat visual cortex: receptive field properties and feature dependence. Eur. J. Neurosci. *2*, 607–619.

Gray, C.M., Konig, P., Engel, A.K., and Singer, W. (1990). Oscillatory responses in cat visual cortex exhibit inter-columnar synchronization which reflects global stimulus properties. Nature *338*, 334–337.

Hansel, D., Mato, G., and Meunier, C. (1993). Phase dynamics for weakly coupled Hodgkin-Huxley neurons. Eurohys. Lett. *23*, 367–372.

Hansel, D., Mato, G., and Meunier, C. (1995). Synchrony in excitatory neural networks. Neural Comput. *7*, 307–337.

Hopfield, J.J. (1995). Pattern recognition computation using action potential timing for stimulus representation. Nature *376*, 33–36.

Hughes, J.R. (1995). The phenomenon of traveling waves: a review. Clin. Electroenceph. *26*, 1–6.

Inoue, T., Wanatnabe, S., Kaywahara, S., and Kirino, Y. (2000).

Phase-dependent filtering of sensory information in the oscillatory olfactory center of a terrestrail mollusk. J. Neurophysiol. *84*, 1112–1115.

Jones, R., Pinto, D., Kaper, T., and Kopell, N. (2000). Alpha-frequency rhythms desynchronize over long cortical distances: a modelling study. J. Comp. Neurosci. *9*, 478–507.

Kawahara, S., Toda, S., Suzuki, Y., Watanabe, S., and Kirino, Y. (1997). Comparative study on neural oscillation in the procerebrum of the terrestrial slugs Incilaria bilineata and Limax marginatus. J. Exp. Biol. *200*, 1851–1861.

Kelso, J.A.S. (1995). Dynamic Patterns: The Self-Organization of Brain and Behavior (Cambridge, MA: MIT Press).

Kleinfeld, D., Delaney, K.R., Fee, M.S., Flores, J.A., Tank, D.W., and Gelperin, A. (1994). Dynamics of propagating waves in the olfactory network of a terrestrial mollusk: an electrical and optical study. J. Neurophysiol. *72*, 1402–1419.

Konig, P., Engle, A.K., Roelfsema, P.R., and Singer, W. (1995). How precise is neuronal synchronization? Neural Comput. *7*, 469–485.

Kopell, N., and Ermentrout, G.B. (1986). Symmetry and phaselocking in chains of weakly coupled oscillators. Comm. Pure Appl. Math. *39*, 623–660.

Kuramoto, Y. (1984). Chemical Oscillations, Waves and Turbulence (New York: Springer Verlag).

Lam, Y.-W.L., Cohen, L.B., Wachowiak, M., and Zochowski, M.R. (2000). Odors elicit three different oscillations in the turtle olfactory bulb. J. Neurosci. *20*, 749–762.

Lampl, I., and Yarom, Y. (1993). Subthreshold oscillations of the membrane potential: a functional synchronizing and timing device. J. Neurophysiol. *70*, 2181–2186.

Lopes da Silva, F.H., and Storm van Leeuwen, W. (1978). The cortical alpha rhythm in the dog: the depth and surface profile of phase. In Architecture of the Cerebral Cortex, M.A. Brazier and M. Petsche, eds. (New York: Raven Press), pp. 319–333.

Macrides, F., Eichenbaum, H.B., and Forbes, W.B. (1982). Temporal relationship between sniffing and the limbic theta rhythm during odor discrimination reversal learning. J. Neurosci. *2*, 1705–1717.

Marder, E., and Calabrese, R.L. (1996). Principles of rhythmic motor pattern generation. Physiol. Rev. *76*, 687–717.

Markram, H., Lubke, J., Frotscher, M., and Sakmann, B. (1997). Regulation of synaptic efficacy by coincidence of postsynaptic APs and EPSPs. Science *275*, 213–215.

Mellon, D., and Wheeler, C.J. (1999). Coherent oscillations in membrane potential synchronize impulse bursts in central olfactory neurons of crayfish. J. Neurophysiol. *81*, 1231–1241.

Murthy, V.N., and Fetz, E.E. (1992). Coherent 25- to 35-Hz oscillations in the sensorimotor cortex of awake behaving monkeys. Proc. Natl. Acad. Sci. USA *89*, 5670–6574.

Neltner, L., Hansel, D., Mato, G., and Meunier, C. (2000). Synchrony in heterogeneous networks of spiking neurons. Neural Comput. *12*, 1607–1641.

Nikitin, E.S., and Balaban, P.M. (1999). Optical recording of odor-evoked responses in olfactory part of the brain of terrestrial mollusk helix. Z. Vysshei Nervnoi Deyatelnosti Imeni I P Pavlov *49*, 817–829.

Paullet, J.E., and Ermentrout, G.B. (1994). Stable rotating waves in two-dimensional discrete active media. SIAM J. Appl. Math. *54*, 1720–1744.

Prechtl, J.C., Cohen, L.B., Mitra, P.P., Pesaran, B., and Kleinfeld, D. (1997). Visual stimuli induce waves of electrical activity in turtle cortex. Proc. Natl. Acad. Sci. USA *94*, 7621–7626.

Prechtl, J.C., Bullock, T.H., and Kleinfeld, D. (2000). Direct evidence for local oscillatory current sources and intracortical phase gradients in turtle visual cortex. Proc. Natl. Acad. Sci. USA *97*, 877–882.

Reyes, A.D., and Fetz, E.E. (1993). Effects of transient depolarizing potentials on the firing rate of cat neocortical neurons. J. Neurophysiol. *69*, 1673–1683.

Ribary, U., Ioannides, A., Singh, K., Hasson, R., Bolton, J., Lado, F., Mogilner, A., and Llinas, R. (1991). Magnetic field tomography of coherent thalamocortical 40-Hz oscillations in humans. Proc. Natl. Acad. Sci. USA *88*, 11037–11041.

Roelfsema, P.R., Engel, A.K., Konig, P., and Singer, W. (1997). Visuomotor integration is associated with zero time-lag synchronization among cortical areas. Nature *385*, 157–161.

Sanchez-Vives, M.V., and McCormick, D.A. (2000). Cellular and network mechanisms of rhythmic recurrent activity in neocortex. Nat. Neurosci. *3*, 1027–1034.

Sanes, J.N., and Donoghue, J.P. (1993). Oscillations in local field potentials of the primate motor cortex during voluntary movement. Proc. Natl. Acad. Sci. USA *90*, 4470–4474.

Schuster, H.G., and Wagner, P. (1990). A model for neuronal oscillations in the visual cortex. II. Phase description of the feature dependent synchronization. Biol. Cybern. 64. 83–85.

Semba, K., and Komisaruk, B.R. (1978). Phase of the theta wave in relation to different limb movements in awake rats. Electroenceph. Clin. Neurophysiol. *44*, 61–71.

Sompolinsky, H., and Tsodyks, M. (1994). Segmentation by a network of oscillators with memory. Neural Comput. *6*, 642–657.

Sompolinsky, H., Golomb, D., and Kleinfeld, D. (1990). Global processing of visual stimuli in a neural network of coupled oscillators. Proc. Natl. Acad. Sci. USA *87*, 7200–7204.

Sompolinsky, H., Golomb, D., and Kleinfeld, D. (1991). Cooperative dynamics in visual processing. Phys. Rev. A *43*, 6990–7011.

Van Vreeswijk, C., Abbott, L.F., and Ermentrout, G.B. (1994). When inhibition not excitation synchronizes neural firing. J. Comp. Neurosci. *4*, 313–321.

von der Malsberg, C., and Schneider, W. (1986). A neural cocktail-party processor. Biol. Cybern. *54*, 29–40.

Wang, D., and Terman, D. (1997). Image segmentation based on oscillatory correlation. Neural Comp. *9*, 805–836.

Watanabe, S., Kawahara, S., and Kirino, Y. (1998). Morphological characterization of the bursting and nonbursting neurones in the olfactory centre of the terrestrial slug Limax marginatus. J. Exp. Biol. *201*, 925–930.

White, J.A., Chow, C.C., Ritt, J., Soto-Trevino, C., and Kopell, N. (1998). Synchronization and oscillatory dynamics in heterogeneous, mutually inhibited neurons. J. Comp. Neurosci. *5*, 5–16.

Whittington, M.A., Traub, R.D., and Jefferys, J.G. (1995). Synchronized oscillations in interneuron networks driven by metabotropic glutamate receptor activation. Nature *373*, 612–615.

Whittington, M.A., Stanford, I.M., Colling, S.B., Jefferys, J.G., and Traub, R.D. (1997). Spatiotemporal patterns of gamma frequency oscillations tetanically induced in the rat hippocampal slice. J. Physiol. *502*, 591–607.

Williams, T.L., and Bowtell, G. (1997). The calculation of frequency-shift functions for chains of coupled oscillations, with application to a network model of the lamprey locomotion pattern generator. J. Comp. Neurosci. *4*, 47–55.